The effects of somatic mutations on EGFR interaction with anti-EGFR monoclonal antibodies: Implication for acquired resistance

Maryam Tabasinezhad[1] Eskanadr Omidinia[2] Yeganeh Talebkhan[1]
Mir Davood Omrani[3] Fereidoun Mahboudi[1] Hamid Ghaedi[3] Wolfgang Wenzel[4]

[1]Biotechnology Research Center, Pasteur Institute of Iran, Tehran, Iran
[2]Department of Genetics and Metabolism, Pasteur Institute of Iran, Tehran, Iran
[3]Medical Genetics Department, School of Medicine, Shahid Beheshti University of Medical Sciences, Tehran, Iran
[4]Institute of Nanotechnology, Karlsruhe Institute of Technology, Karlsruhe, Germany

Correspondence
Fereidoun Mahboudi, Biotechnology Research center, Pasteur Institute of Iran, 12 Farvardin Ave., Enghelab Square, Tehran, Iran.
Email: mahboudif@cinnagen.com

Hamid Ghaedi, Department of Medical Genetics, School of Medicine, Shahid Beheshti University of Medical Sciences, Velenjak St., Shahid Chamran Highway, Tehran, Iran.
Email: h.qaedi@sbmu.ac.ir

Funding information
Pasteur Institute of Iran, Grant/Award Number: BP 9146

Abstract

A number of mutations in the epidermal growth factor receptor (EGFR) have been identified that imparts resistance to anti-EGFR monoclonal antibodies (mAbs) in clinical and preclinical samples. Primary or acquired resistance to targeted therapy will eventually limit the clinical benefit of anticancer mAbs. The aim of the current study was to perform computational analysis to investigate the structural implications of the EGFR somatic mutations on its complexes with the four anti-EGFR mAbs (Cetuximab, Panitumumab, Necitumumab, and Matuzumab). Docking analysis and molecular dynamics (MD) simulations were performed to understand the plausible structural and dynamical implications caused by somatic mutations available in the Catalogue of Somatic Mutations in Cancer database on the EGFR and anti-EGFR mAbs. We found that $EGFR^{S492R}$ and $EGFR^{V441I}$ in complex with Cetuximab, $EGFR^{R377S}$ and $EGFR^{S447Y}$ in complex with Panitumumab, and $EGFR^{V441I}$ in complex with Necitumumab have a weakest binding affinity in comparison to $EGFR^{WT}$ in complex with the relevant mAb. Taken together with the results obtained from docking analysis and MD simulations, the present findings may suggest that, the S492R and V441I mutations confer resistance to Cetuximab, R377S and S447Y mutations mediate resistance to Panitumumab and finally, V441I mutation also confers resistance to Necitumumab.

KEYWORDS
Cetuximab, EGFR, in silico, Matuzumab, mutation, Necitumumab, Panitumumab

1 INTRODUCTION

The epidermal growth factor receptor (EGFR) is widely expressed in human tissues and modulates key cellular processes including proliferation, differentiation, and apoptosis. In oncology setting, EGFR is the first molecular target against which monoclonal antibodies (mAbs) have been developed for targeted therapy.[1,2] There are different types of therapeutic anti-EGFR mAbs including but not limited to Cetuximab, Panitumumab, Matuzumab, and Necitumumab.[3] Plethoras of evidence suggest the efficacy of these mAbs in treating a range of cancers including lung and colon cancer.[4] It has previously been observed that primary or acquired resistance to anti-EGFR antibody therapies can arise through different mechanisms including acquired secondary mutations. These mutations may occur in the EGFR ectodomain or downstream signaling molecules such as KRAS and NRAS.[5] As a consequence, acquired resistance to targeted therapy will eventually limit the clinical benefit of anticancer mAbs.

Recently, a number of studies have investigated the molecular mechanisms underlying resistance to anti-EGFR mAbs. Up to now, limited number of mutations in the EGFR has been described that

imparts resistance to Cetuximab and Panitumumab in clinical and preclinical samples.[6,7] Montagut et al[6] discovered that cell lines with acquired resistance to Cetuximab showed S492R mutation of the EGFR extracellular domain. This mutation can be acquired during therapy with Cetuximab and confers resistance to this antibody, yet amazingly remains sensitive to Panitumumab. Moreover, there are additional mutations in the EGFR that also shown cross-resistance profiles to both Panitumumab and Cetuximab.[7] It has become clear that such mutations abrogate the EGFR binding to anti-EGFR mAbs.

Given the fact that mutations in the EGFR ectodomain may lead to a difference in treatment response, the specific objective of this study was to identify somatic mutations from the Catalogue of Somatic Mutations in Cancer (COSMIC) database,[8] that resided within EGFR ectodomain and then computationally investigate the effects of these mutations on the EGFR and anti-EGFR mAbs interaction.

2 MATERIALS AND METHODS

Figure 1 depicts the overall approach employed in this study. Briefly, somatic mutations from the COSMIC database[8] have been mapped to the EGFR ectodomain (361-480 aa), to obtain a dataset containing point mutations within the EGFR epitopes. Moreover, we included a previously identified resistance-conferring mutation S492R in our analysis, to check whether or not the applied protocol could identify this mutation as Cetuximab resistance-conferring variant. Further, we used PyMol to generate a library of EGFR mutant models. Finally, interactions of the EGFR mutants and relevant anti-EGFR mAbs were evaluated and characterized by docking and molecular dynamics (MD) simulations.

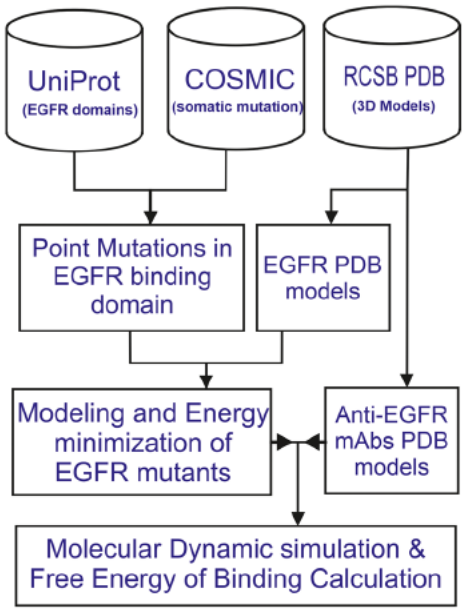

FIGURE 1 Schematic representation of the study workflow. EGFR, epidermal growth factor receptor [Color figure can be viewed at wileyonlinelibrary.com]

3 DATASETS COLLECTION

We downloaded somatic mutations of the EGFR from the COSMIC v85.[8] We considered single nucleotide substitutions for further analysis. The amino acid sequence and details of the human EGFR domains (P00533) were obtained from the UniProt database.[9] The X-ray crystallographic structures for EGFR complex with Cetuximab (PDB ID: 1YY9), Panitumumab (PDB ID:5SX5), Matuzumab (PDB ID: 3C09), and Necitumumab (PDB ID: 6B3S) were obtained from the Research Collaboratory for Structural Bioinformatics (RCSB) PDB.[10]

With regard to the list of mutations resided within the EGFR ectodomain, we used the PyMol software to mutate the wild-type EGFR molecule (PDB ID: 3QWQ) into mutant forms. Subsequently, the mutant models were subjected to an energy minimization protocol by the GROMACS toolkit using the steepest descent algorithm.[11]

4 DOCKING ANALYSIS

In order to predict interactions between EGFR models and relevant mAbs, docking was performed by ClusPro web server.[12] It is one of the most widely used server for predicting antibody-antigen interactions and ranked first in the last CAPRI (Critical Assessment of PRedicted Interactions) evaluation meeting in April 2016. Motivated by the CAPRI, through the last 2 years, ClusPro server has been substantially improved to perform ultrafast docking with considerable precision.[13] The web server provides two platforms DOT and ZDOCK to perform rigid-body docking and the both of which are based on the fast Fourier transform (FFT) correlation techniques. It is well accepted that FFT based algorithms are the key principle of rigid-body protein docking procedures.[12] In this study, we selected DOT platform for docking as it considers the electrostatic potential and surface complementarity between the two structures. This would help in the preservation of the structures with fine conformations. Two parameters, distance-dependent electrostatics and empirical potential energy scores were considered to filter the obtained structures. In the case of each antibody, top five complexes with more positive docking energy were selected for further analysis by MD simulation as the initial conformations.

5 MD SIMULATION

Molecular dynamics simulation was performed by using the GROMACS 5.1.4 package with the original GROMOS96 force field 43A1.[11] The complex structure of wild-type/mutants EGFR and mAbs were served as starting point for MD simulation. Antibody-antigen complexes were solvated in a rectangular box with SPC/E water molecules with a 10 Å marginal radius. Simulations were carried out using periodic boundary conditions and particle mesh Ewald method to consider the long-range electrostatic interactions. In order to make the simulation system electrically neutral, we replaced solvent molecules with Cl^- or Na^+ ions. Then, the system was

relaxed using the steepest descent energy minimization algorithm while the maximum force was set to 1000.00 kJ mol^{-1} nm^{-1}.

After energy minimization, the system was equilibrated for 500 ps using NVT (constant number of particles, system volume, and temperature), and another 500 ps by NPT (constant number of particles, system pressure, and temperature) which ensembles at 300 K.

After 5000 iterations of energy minimization steps, the entire system was equilibrated for 500 ps using canonical NVT and isothermal-isobaric NPT which ensembles at 300 K. To constrain the lengths of all bonds including hydrogen atoms, the algorithm LINCS constraint was employed. We considered a cut-off of 1 nm for the calculation of Coulomb and van der Waals (VdW) interactions. At the final step, equilibrated systems were simulated for 50 ns at 300 K with 2 fs time step. The result trajectories were used for further processing. We used GROMACS analysis toolkit in order to analyze MD trajectories generated during the production run to calculate the root mean square deviation (RMSD). For graphs visualization, various software including Microsoft Excel 2016, GraphPad Prism (release 8.0.0, GraphPad Software, San Diego, California), and Xmgrace (Grace 5.1.21)[14] was used.

The free energy of binding (ΔG) was approximated using the Molecular Mechanics Poisson-Boltzmann Surface Area (MMPBSA) method using MMPBSA.py implemented in AmberTools.[15]

For the calculation of free energy of binding (binding affinity), VdW energy, electrostatic energy, surface accessible surface area, and polar solvation energy, we used GROMACS Molecular Mechanics Poisson-Boltzmann Surface Area (G MMPBSA) method implemented in GROMACS 5.1.4.[16] A total of 2000 snapshots structures extracted from 50 000 frames of the MD runs, were used for the calculation of free energy of binding (ΔG_{bind}) using the equations as described by Kumari et al.[16]

6 VISUALIZATION OF INTERACTION SURFACE

The EGFRs and mAbs were visualized using the PyMol software. We used APBS (Adaptive Poisson-Boltzmann Solver) tool,[17] to visualize interaction surface of the complexes. It is the PyMOL plugin software which evaluates the electrostatic characteristics of nanoscale biomolecular systems, by a solution of the Poisson-Boltzmann equation. The APBS tool takes a .pqr and a .in file as input. It estimates the electrostatic potential in all points of a grid in the protein space and finally visualizes the electrostatic potential of a protein complex. In order to generate .pqr files, we used PDB2PQR-2.0.0 web server.[18] This server provides a platform-independent utility for changing protein files from .pdb format to .pqr format. PDB2PQR allocates partial atomic charge to all atoms according to different force fields (AMBER 94, CHARMM 27, or PARSE) and records output as a .pqr file. The .in file retains information on the 3D dimension of the protein complex, the solvent ionic concentration, and dielectric constants of biomolecular and solvent.

7 RESULTS

7.1 Primary datasets characteristics

The EGFR protein is 1210 aa in length and data from UniProt for EGFR HUMAN (P00533) molecule suggested that it has consisted of five distinct domains and three Furin-like repeats. We called the "Receptor L-domain" that span from residue 361 to 480, as ectodomain. In this study, the ectodomain is defined as the domain that involved in the interaction with mAbs. We retrieved all mutations resided within the EGFR from the COSMIC v85 database (Figure 2). As listed in Table 1,

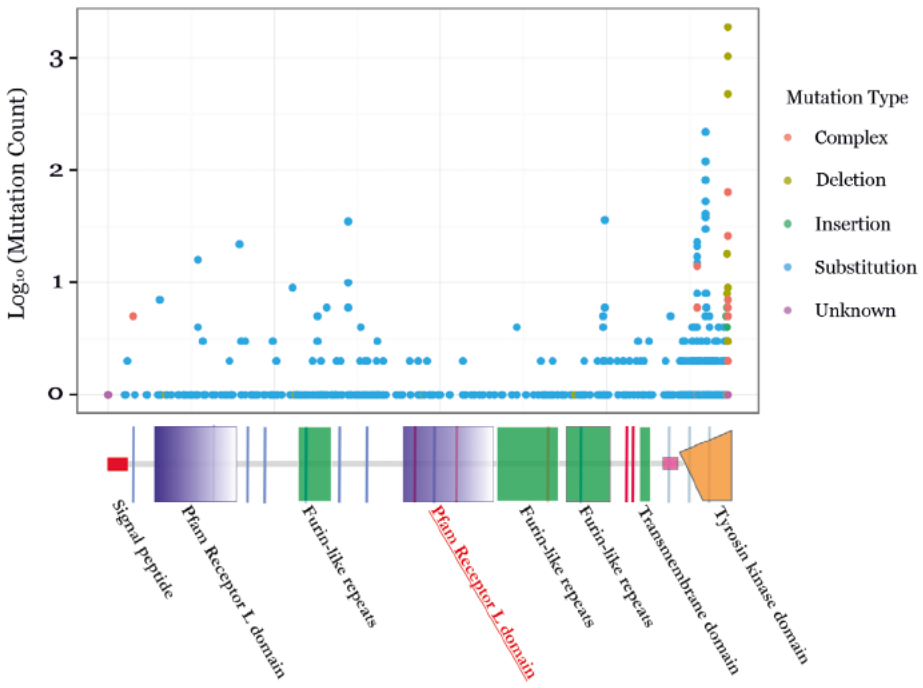

FIGURE 2 The mutational pattern across different domains and repeats of the EGFR. The ectodomain is indicated Receptor L domain in red. EGFR, epidermal growth factor receptor [Color figure can be viewed at wileyonlinelibrary.com]

TABLE 1 The list of missense mutations within the EGFRectodomain

No.	Position (aa)	Mutation	No.	Position (aa)	Mutation
1	363	p.T363I	13	427	p.R427L
2	364	p.S364F	14	430	p.T430I
3	375	p.A375T	15	437	p.S437Y
4	377	p.R377S	16	441	p.V441I
5	384	p.T384S	17	447	p.S447Y
6	387	p.L387 M	18	451	p.R451F
7	387	p.L387 V	19	459	p.G459A
8	390	p.Q390K	20	465	p.G465R
9	397	p.T397S	21	473	p.N473D
10	400	p.E400K	22	475	p.I475V
11	411	p.P411R	23	492	p.S492R[a]
12	427	p.R427C			

Abbreviation: EGFR, epidermal growth factor receptor.
[a]This mutation is not resided within the EGFR ectodomain, but still is located in the EGFR binding site.

the study was limited to investigate missense mutations found in the EGFR ectodomain (n = 22) and S492R variant.

7.2 Modeling and docking analysis result

Docking of the wild-type EGFR and 23 EGFR mutant models with four anti-EGFR mAbs including Cetuximab, Panitumumab, Matuzumab, and Necitumumab was performed by ClusPro server. We found the lowest energy of binding for $EGFR^{WT}$-Cetuximab, -Panitumumab, -Matuzumab, and -Necitumumab complex was as 1158.4, 900.7, 800.5, and 920.8 kJ/mol, respectively. Further, we showed that several mutations in the case of each antibody unfavorably changed the docking energy of interactions (Figure 3). Data showed out of the 23 mutants, $EGFR^{S492R}$ revealed most positive docking energy in complex with Cetuximab (Figure 3A). The complex of Panitumumab with $EGFR^{R377S}$ identified to be thermodynamically most unfavorable complex as compared to an interaction of this antibody with wild-type EGFR and also other EGFR mutants (Figure 3B). In the case of Matuzumab, data showed that its complex with $EGFR^{G465R}$ mutant has a more positive docking energy

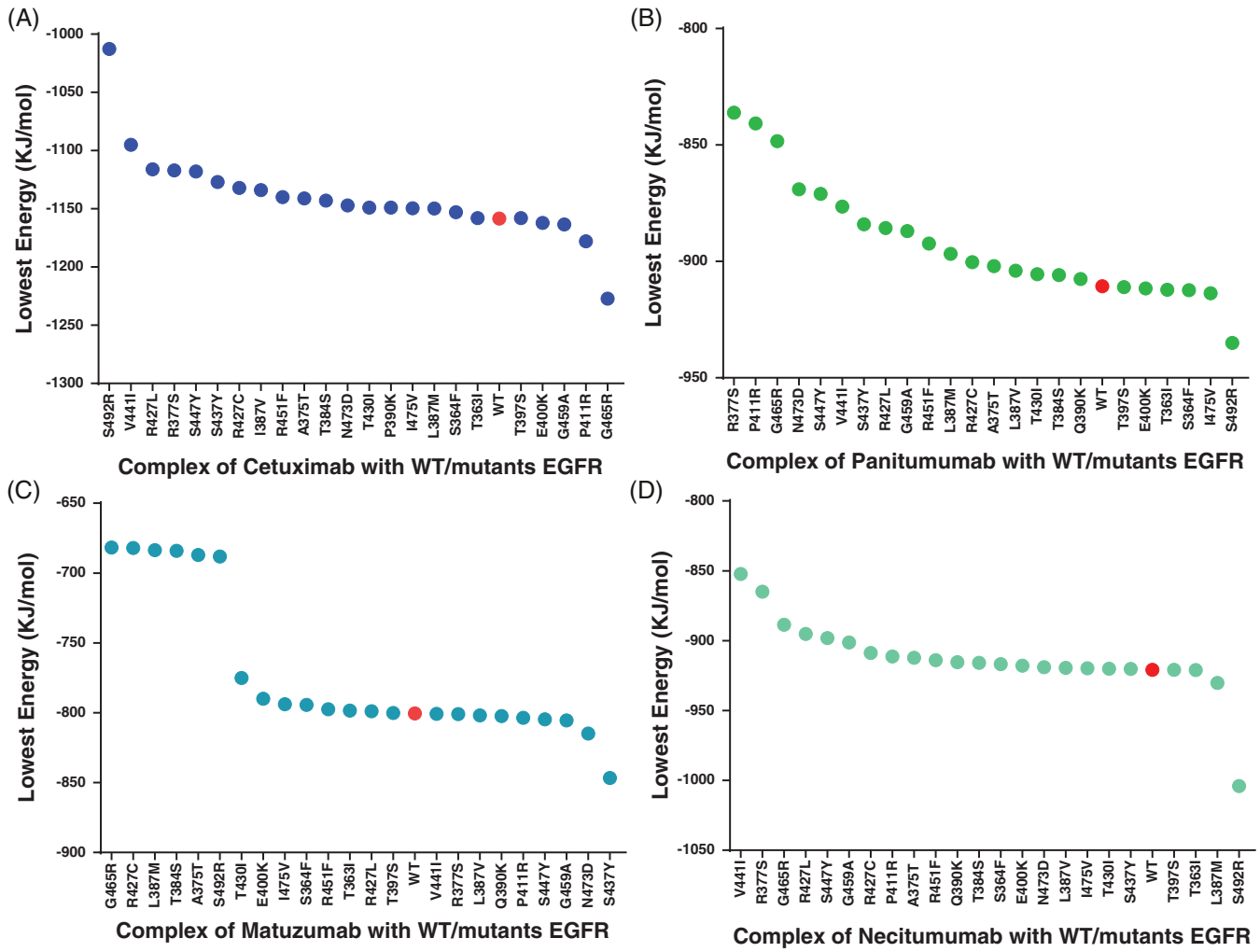

FIGURE 3 Docking energy of native and mutants EGFR with anti-EGFR mAbs. A-D represent docking energy of EGFRs in complex with Cetuximab, Panitumumab, Matuzumab, and Necitumumab, respectively. EGFR, epidermal growth factor receptor [Color figure can be viewed at wileyonlinelibrary.com]

level in comparison with both native and other EGFR mutants (Figure 3C). Of Necitumumab complexes with EGFRs, $EGFR^{V441I}$-Necitumumab was found at the complex with more positive docking energy level (Figure 3D).

7.3 Free energy of binding calculations

The MM/PBSA approach is one of the most widely used methods to calculate the binding free energy of biomolecular complexes. The effectiveness of the G_MMPBSA tool to estimate the relative binding free energy of complexes and also providing a decomposition of the residue contribution to binding has been reported repeatedly.

In the case of each mAb, we selected the top five EGFR mutants which demonstrated most positive docking energy in complex with the relevant mAb for MD simulation. Further, MD trajectories of the complexes at a stable 2 ns interval (from 16 to 18 ns) were extracted and then applied for the free energy of binding calculation with the G_MMPBSA tool. The free energy of binding and its related components resulted from the MMPBSA calculation of the Cetuximab-EGFRs, Panitumumab-EGFRs, Matuzumab-EGFRs, and Necitumumab-EGFRs are presented in Tables 2–5, respectively.

It is worth to mention that the value of free energy of binding affinity by G_MMPBSA indicates a relative change between the WT and mutant models. However, the absolute values for the free energy of binding are challenging to interpret. Depending on the characters of atoms in the EGFR epitopes, a range of different interactions including hydrophobic, hydrogen, electrostatics, and *pi-pi* interactions were formed between the EGFRs and the mAbs residues. These individual components may contribute either favorable or unfavorable impact on the overall binding free energy. We found that the complex of Cetuximab with $EGFR^{V441I}$ or $EGFR^{S492R}$ to have a most positive free energy of binding comparing to Cetuximab-$EGFR^{WT}$ complex (Figure 4A). Also, data showed that both electrostatic and VdW energies increased for the complex of Cetuximab with $EGFR^{V441I}$ and $EGFR^{S492R}$ (Table 2). This could be explained by the evident decrease in the number of hydrogen bonds and hydrophobic interactions at the binding pocket of the mAb/EGFR. Therefore, binding affinity of Cetuximab to EGFR would be decreased significantly when V441I or S492R mutation is present an interaction surface.

As illustrated in Figure 4B, in comparison to Panitumumab-$EGFR^{WT}$, the complex of Panitumumab with $EGFR^{R377S}$ and $EGFR^{S447Y}$ has remarkably more positive values for the free energy of binding. The electrostatic energy of both complexes decreased, however, the reduction is not enough to compensate increasing of VdW energy (Table 3). Therefore, binding affinity of Panitumumab would decrease to interact with both $EGFR^{R377S}$ and $EGFR^{S447Y}$.

Our result indicated that the free binding energy of Necitumumab-$EGFR^{V441I}$ complex is significantly more positive than Necitumumab-$EGFR^{WT}$ complex (Figure 4D). The V441I mutation could lead to a decrease in hydrogen and hydrophobic interaction numbers at a binding site of the complex. This eventually would lead to a positive increase in the VdW and electrostatic energy of the Necitumumab-$EGFR^{V441I}$ complex. Therefore, binding affinity of Necitumumab to EGFR may be decreased whenever Val mutates to Ile at the residue 441.

In the case of Matuzumab, our result indicated that from the mutations inspected in this study, no mutation could decrease the binding affinity of Matuzumab to the EGFR mutant models (Table 4 and Figure 4C).

TABLE 2 The result of G_MMPBSA calculation for free energies of Cetuximab-EGFRs complexes

EGFR type	Van der Waals (kJ/mol)	Electrostatic (kJ/mol)	Polar solvation (kJ/mol)	SASA energy (kJ/mol)	Binding energy (kJ/mol)
$EGFR^{V441I}$	147 851.10 ± 4979.84	468.11 ± 74.65	928.57 ± 119.10	94.47 ± 6.75	148 217.09 ± 4974.187
$EGFR^{S492R}$	147 521.38 ± 4653.25	373.87 ± 106.72	778.96 ± 123.85	85.39 ± 6.94	147 841.06 ± 4654.74
$EGFR^{R377S}$	146 824.02 ± 5065.94	595.11 ± 64.51	965.58 ± 115.32	95.41 ± 6.28	147 099.07 ± 5070.11
$EGFR^{WT}$	146 710.57 ± 4824.06	709.34 ± 88.90	963.48 ± 133.08	98.69 ± 7.22	146 866.01 ± 4820.20
$EGFR^{S447Y}$	146 710.321 ± 4539.41	700.36 ± 90.18	960.864 ± 126.38	109.64 ± 9.47	146 861.185 ± 4985.17
$EGFR^{R427L}$	42 376.94 ± 1348.58	263.72 ± 107.76	572.00 ± 133.62	75.25 ± 7.58	42 609.96 ± 1353.58

Abbreviations: EGFR, epidermal growth factor receptor; SASA, surface accessible surface area.

TABLE 3 The result of G_MMPBSA calculation for free energies of Panitumumab-EGFRs complexes

EGFR type	Van der Waals (kJ/mol)	Electrostatic (kJ/mol)	Polar solvation (kJ/mol)	SASA energy (kJ/mol)	Binding energy (kJ/mol)
$EGFR^{R377S}$	147 476.11 ± 4231.52	719.41 ± 82.76	717.95 ± 121.19	78.18 ± 6.07	147 396.47 ± 4230.92
$EGFR^{S447Y}$	147 286.62 ± 5029.51	851.07 ± 76.94	938.97 ± 108.94	91.28 ± 6.16	147 283.24 ± 5028.53
$EGFR^{G465R}$	147 009.32 ± 4341.63	833.07 ± 414.49	792.32 ± 140.79	92.22 ± 19.50	146 876.34 ± 4354.09
$EGFR^{N473D}$	146 954.69 ± 5139.10	723.23 ± 76.00	726.69 ± 106.45	82.9 ± 6.18	146 875.25 ± 5135.50
$EGFR^{WT}$	146 649.88 ± 4929.72	628.65 ± 90.43	783.47 ± 85.49	93.97 ± 6.29	146 710.73 ± 4936.19
$EGFR^{P411R}$	111 180.52 ± 3634.53	1216.09 ± 99.08	1285.05 ± 132.41	87.70 ± 6.29	111 161.77 ± 643.48

Abbreviations: EGFR, epidermal growth factor receptor; SASA, surface accessible surface area.

TABLE 4 The result of G MMPBSA calculation for free energies of Matuzumab-EGFRs complexes

EGFR type	Van der Waals (kJ/mol)	Electrostatic (kJ/mol)	Polar solvation (kJ/mol)	SASA energy (kJ/mol)	Binding energy (kJ/mol)
$EGFR^{WT}$	147 903.01 ± 5406.20	277.12 ± 56.44	754.87 ± 91.76	41.89 ± 7.46	148 338.87 ± 5409.66
$EGFR^{L387M}$	147 351.55 ± 4662.00	345.99 ± 60.25	826.79 ± 101.08	36.08 ± 7.17	147 796.26 ± 4650.98
$EGFR^{G465R}$	147 282.82 ± 4181.21	306.16 ± 97.19	729.44 ± 151.56	33.98 ± 7.40	147 672.12 ± 4187.71
$EGFR^{R427C}$	147 069.20 ± 4618.36	283.04 ± 72.92	712.02 ± 119.41	41.58 ± 7.54	147 456.59 ± 4633.51
$EGFR^{A375T}$	146 886.549 ± 4428.74	391.37 ± 65.28	557.04 ± 128.38	39.48 ± 7.06	147 012.74 ± 4340.41
$EGFR^{T384S}$	146 605.138 ± 4687.64	160.715 ± 78.35	508.592 ± 117.39	32.872 ± 7.89	146 920.143 ± 4265.16

Abbreviations: EGFR, epidermal growth factor receptor; SASA, surface accessible surface area.

TABLE 5 The result of G MMPBSA calculation for free energies of Necitumumab-EGFRs complexes

EGFR type	Van der Waals (kJ/mol)	Electrostatic (kJ/mol)	Polar solvation (kJ/mol)	SASA energy (kJ/mol)	Binding energy (kJ/mol)
$EGFR^{V441I}$	147 184.22 ± 5039.10	313.63 ± 98.76	523.76 ± 119.32	72.43 ± 6.74	147 322.65 ± 5234.19
$EGFR^{R377S}$	146 953.26 ± 4829.70	415.63 ± 74.14	729.11 ± 146.86	84.48 ± 6.32	147 192.45 ± 4779.86
$EGFR^{WT}$	146 719.48 ± 4391.80	536.11 ± 69.78	1056.56 ± 151.4	94.73 ± 6.81	147 145.39 ± 4682.43
$EGFR^{R427L}$	146 867.11 ± 4580.35	134.28 ± 54.83	912.94 ± 124.90	42.33 ± 6.97	146 949.41 ± 4938.74
$EGFR^{S447Y}$	146 220.14 ± 4611.30	319.85 ± 67.43	773.19 ± 117.39	90.88 ± 6.14	146 583.89 ± 4847.10
$EGFR^{G465R}$	145 941.68 ± 4362.76	299.34 ± 56.46	757.61 ± 134.74	90.45 ± 6.48	146 309.47 ± 4687.36

Abbreviations: EGFR, epidermal growth factor receptor; SASA, surface accessible surface area.

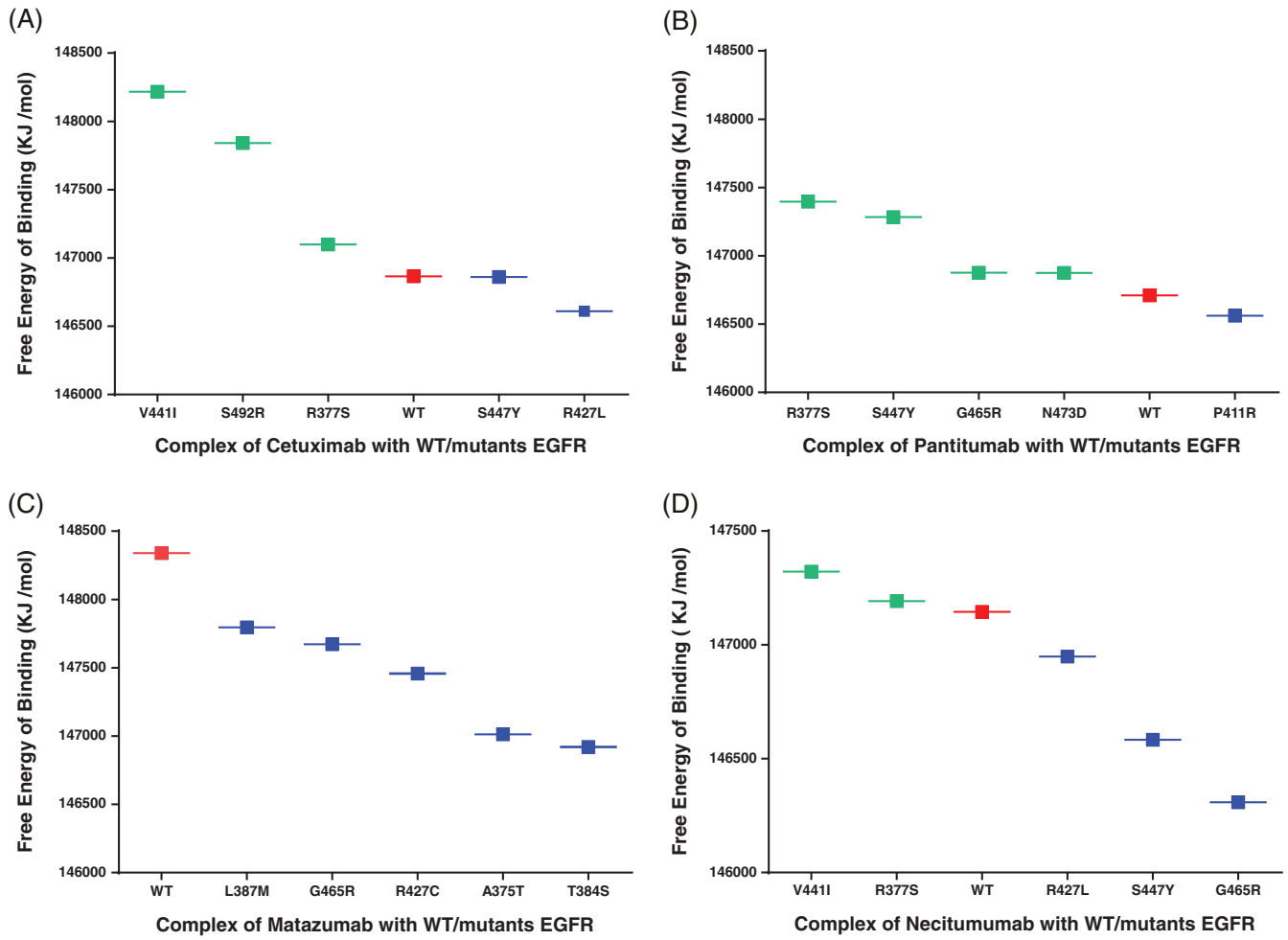

FIGURE 4 The free energy of binding of the mAbs in complex with different EGFR mutant models. A-D represent the free energy of binding of EGFRs in complex with Cetuximab, Panitumumab, Matuzumab, and Necitumumab, respectively. EGFR, epidermal growth factor receptor [Color figure can be viewed at wileyonlinelibrary.com]

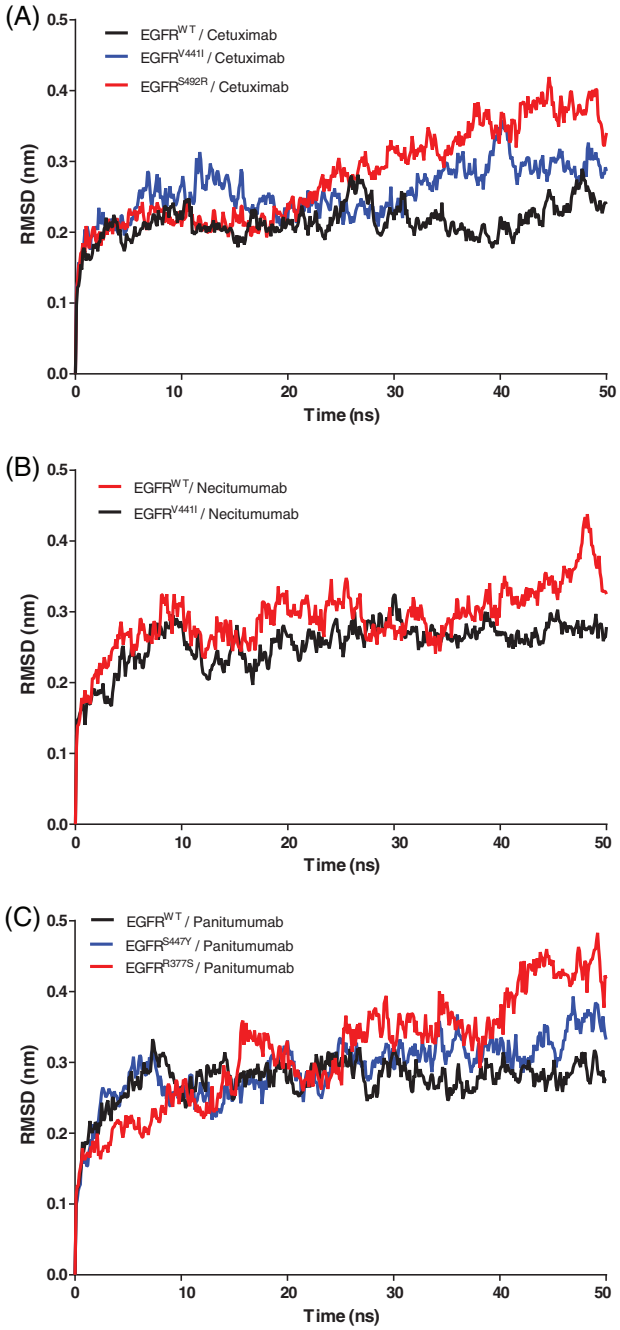

FIGURE 5 Root mean square deviation of anti-EGFR mAbs complexes with mutant EGFRs along the MD simulation. A–C represent RMSD plot of Cetuximab-EGFRs, Panitumumab–EGFRs, and Necitumumab-EGFRs, respectively. EGFR, epidermal growth factor receptor; MD, molecular dynamics; RMSD, root mean square deviation

7.4 Stability of mAb-EGFR complexes

To gain further insights into the structural effect of the mutations which significantly decreased binding affinity, the stability of EGFR-anti-EGFR complexes were predicted by RMSD analysis.

The RMSD values of the Cetuximab-EGFR^{S492R}, Cetuximab-EGFR^{V441I}, Panitumumab-EGFR^{R377S}, Panitumumab-EGFR^{S447Y}, and Necitumumab-EGFR^{V441I} backbone atoms relative to these mAbs in complex with EGFR^{WT} were measured (Figure 5). All of the complexes reached equilibrium after 10 ns of the simulation phase. This indicated that the trajectories of the MD simulations for all of the complexes next to equilibrium are reliable for further assessments. The RMSD of EGFR^{WT}, EGFR^{S492R}, and EGFR^{V441I} in complex with Cetuximab is under 0.3 nm until 30 ns with a slight increase in the RMSD value of the EGFR^{S492R} and EGFR^{V441I}. However, after 30 ns a noticeable deviation in the backbone RMSD value of these mutant complex structures is evident. The RMSD value of the mutants continued to increase more than 0.4, although the RMSD value of EGFR^{WT} was drop down to 0.2 nm until 50 ns (Figure 5A). Our findings suggested that mutation of Ser492 to Arg and mutation of Val441 to Ile could potentially destabilize EGFR interaction with Cetuximab.

As Figure 5B illustrates, RMSD values of EGFR^{WT}, EGFR^{R377S}, and EGFR^{S447Y} in complex with Panitumumab are about 0.3 nm until 30 ns. One can see that for EGFR^{WT}-Panitumumab complex, the maximum RMSD value reached a level of about 0.3 nm, while for the EGFR^{R377S}- and EGFR^{S447Y}-Panitumumab complexes, RMSD values exceeded to 0.3 nm, and in the case of EGFR^{R377S}-Panitumumab, the value reached a level of 0.5 nm until 50 ns. Our result evidenced that S447Y and R377S mutations in the EGFR could change the interaction of epitopes with Panitumumab and consequently reduced the stability of the complexes.

The RMSD value of EGFR^{WT}- and EGFR^{V441I}-Necitumumab was about 0.3 nm until 40 ns (Figure 5C). After this time point, RMSD value of EGFR^{V441I}-Necitumumab started to increase and finally reached 0.4 nm at 50 ns. Such findings suggest a destabilizing effect of V441I substitution on the EGFR interaction with Necitumumab.

7.5 Interaction surface analysis

In order to obtain deeper insights into the effects of the mutations with unfavorable consequences (decreasing both mAb-EGFR complexes stability and binding affinity) on the mAbs-EGFR complex, we performed a close inspection on their interactions at the binding pockets of the mAb-EGFR complexes.

We found that Ser492 residue of EGFR^{WT} is involved in hydrophobic interactions with Trp94 on the light chain of Cetuximab (Figure 6A,B). Substitution of Ser492 with Arg on the ectodomain of EGFR (Figure 6D) significantly changed the binding pose of EGFR^{S492R} from hydrophilic negatively charged (Figure 6A) to a high positive surface potential region (Figure 6C). Since there is a difference in charge between the Ser and Arg amino acid, the S492R mutation introduces a positive charge at this position. Consequently, this can cause repulsion between the mutant residue and neighboring residues at the binding pocket.

The mutation of Val441 to Ile (Figure 7B,D) could increase positive surface potential at the binding pose of EGFR^{V441I} (Figure 7A,C). These alterations on the surface of EGFR would lead to a weaker nonpolar and dispersion forces with Tyr102 on the heavy chain of Cetuximab.

Substitution of Arg377 with Ser on the EGFR extended a negatively charged hydrophilic surface on the region (Figure 8A,C). The

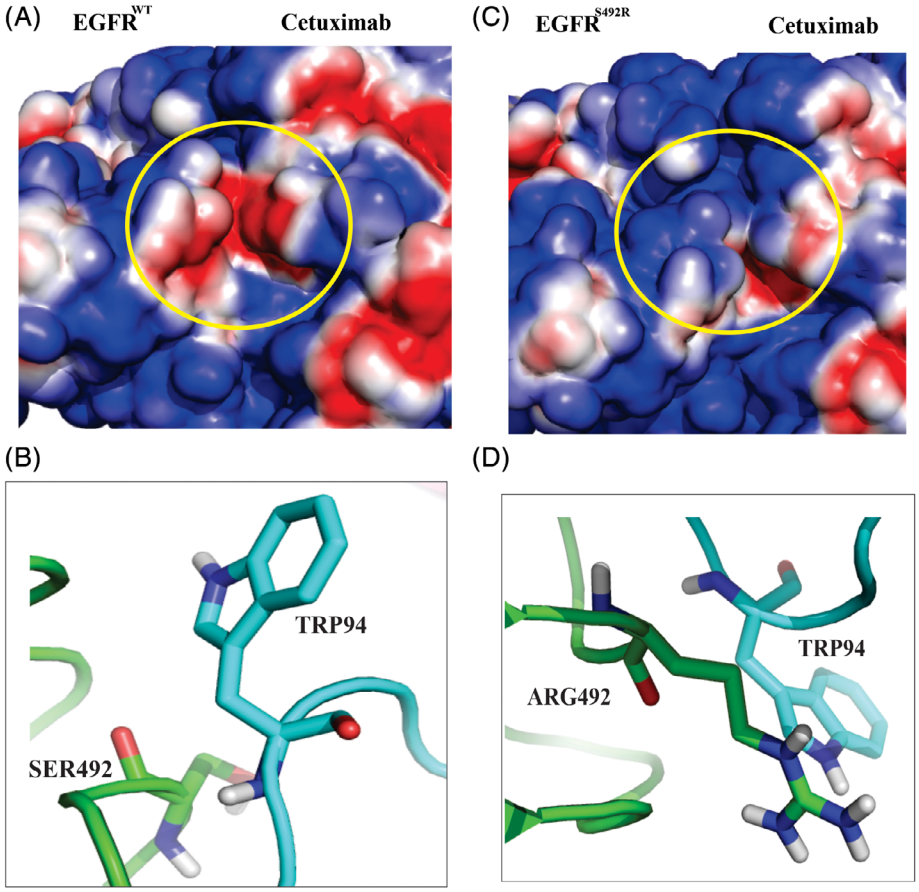

FIGURE 6 Conformation change of EGFR binding poses for Cetuximab as a result of S492R mutation occurrence. A and C are a representation of the interaction surface for $EGFR^{WT}$- and $EGFR^{S492R}$-Cetuximab, respectively. B represents amino acid interactions at binding sites of $EGFR^{WT}$ in complex with Cetuximab. D represents amino acid interactions at binding sites of $EGFR^{S492R}$ in complex with Cetuximab which the interaction of $EGFR^{WT}$-Cetuximab would disturb by the S492R mutation. EGFR, epidermal growth factor receptor [Color figure can be viewed at wileyonlinelibrary.com]

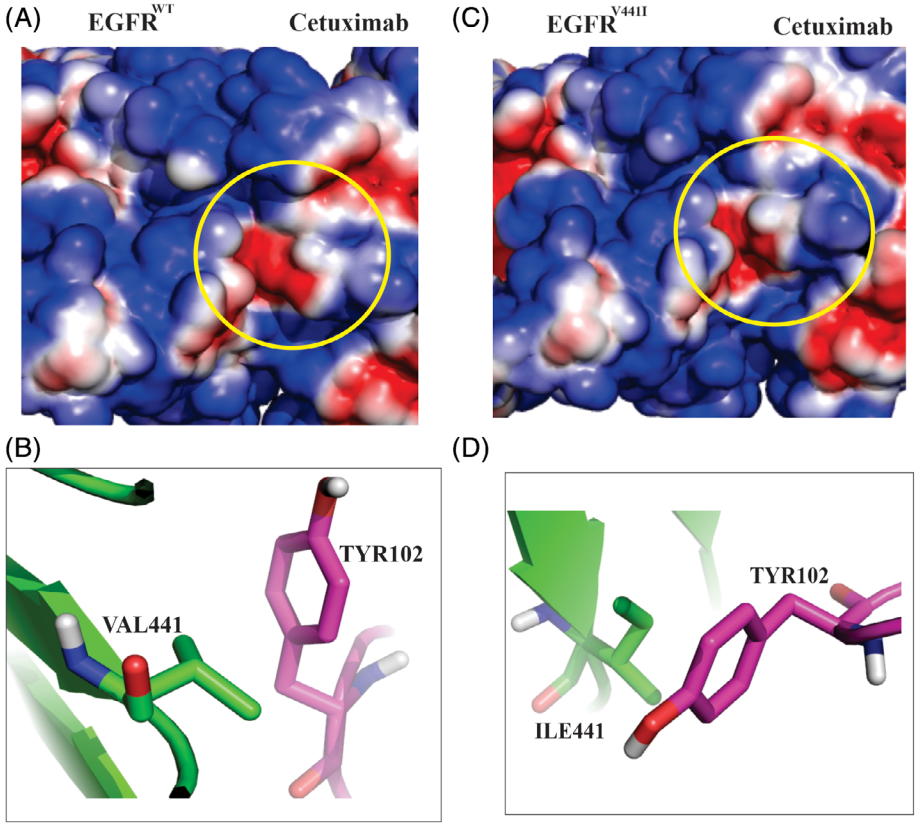

FIGURE 7 Conformation change of the EGFR binding site for Cetuximab due to V441I mutation. A and C are the representation of the interaction surface for $EGFR^{WT}$- and $EGFR^{V441I}$-Cetuximab, respectively. B represents amino acid interactions at the binding sites of $EGFR^{WT}$ in complex with Cetuximab. D represents amino acid interactions at binding sites of $EGFR^{V441I}$ in complex with Cetuximab which the interaction of $EGFR^{WT}$-Cetuximab would disturb by the V441I mutation. EGFR, epidermal growth factor receptor [Color figure can be viewed at wileyonlinelibrary.com]

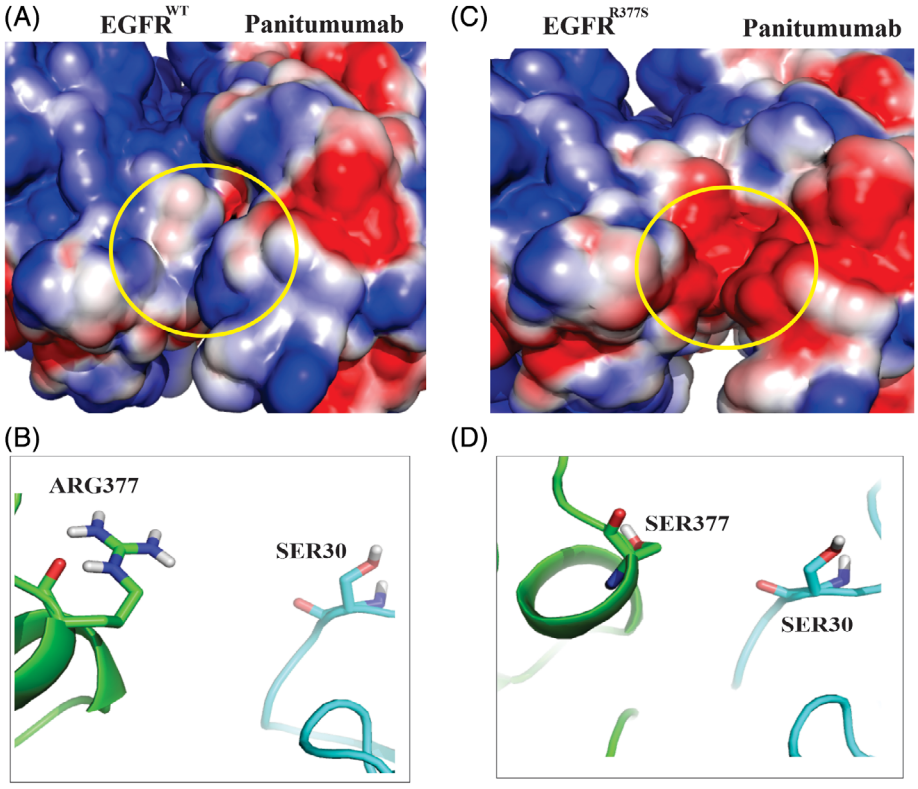

FIGURE 8 Conformation change of the EGFR binding site for Panitumumab because of R377S mutation. A and C are the representation of interaction surface for $EGFR^{WT}$- and $EGFR^{R377S}$-Panitumumab, respectively. B represents amino acid interaction at the binding sites of $EGFR^{WT}$ in complex with Panitumumab. D represents amino acid interactions at binding sites of $EGFR^{R377S}$ in complex with Panitumumab which the interaction of $EGFR^{WT}$-Panitumumab would disturb by the R377S mutation. EGFR, epidermal growth factor receptor [Color figure can be viewed at wileyonlinelibrary.com]

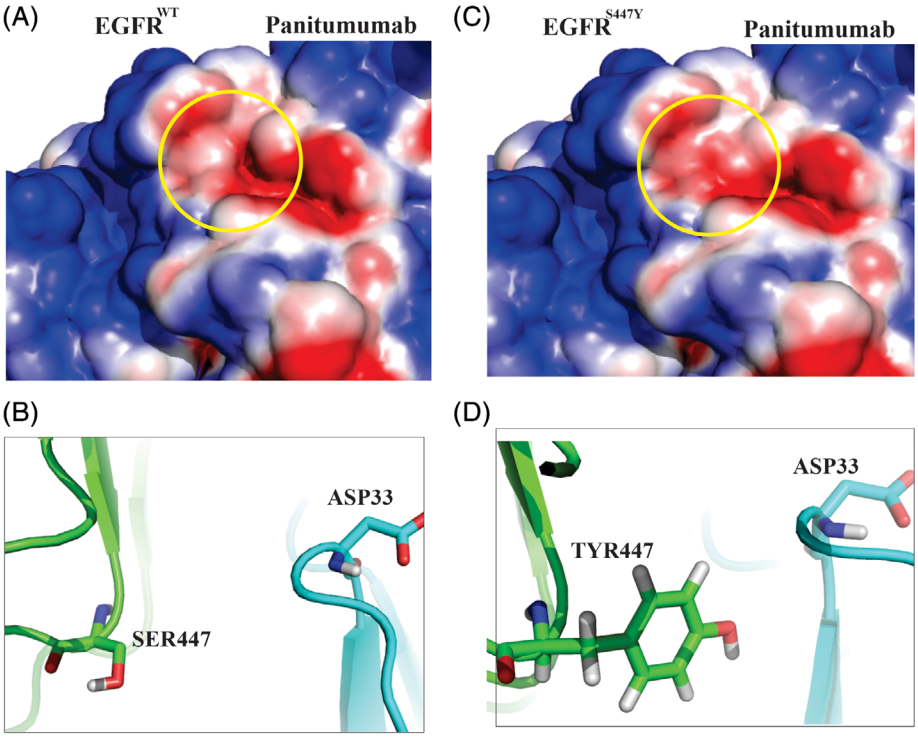

FIGURE 9 Conformation change of the EGFR binding site for Panitumumab due to S447Y mutation. A and C are the representation of the interaction surface for $EGFR^{WT}$- and $EGFR^{S447Y}$-Panitumumab, respectively. B represents amino acid interaction at the binding sites of $EGFR^{WT}$ in complex with Panitumumab. D represents amino acid interactions at binding sites of $EGFR^{S447Y}$ in complex with Panitumumab which the interaction of $EGFR^{WT}$-Panitumumab would disturb by the S447Y mutation. EGFR, epidermal growth factor receptor [Color figure can be viewed at wileyonlinelibrary.com]

modification at the binding interaction of $EGFR^{R377S}$, contributed to disturb interaction of Arg377 of $EGFR^{R377S}$ with Ser30 on the light chain of Panitumumab (Figure 8B,D) and decreased the electrostatic interactions. The difference in the charge between wild-type and mutant residue will disturb the ionic interaction made by the original, wild-type residue.

As a consequence of Ser447 mutation to Tyr on EGFR, a phenol group is introduced at this position (Figure 9B,D). This partially changes the electrostatic surface potential of the antigen binding site (Figure 9A,C) and it would decrease strong electrostatic interactions of EGFR with Panitumumab. Also the wild-type residue, Ser447 forms a hydrogen bond with Asp at position 416 of EGFR. The size

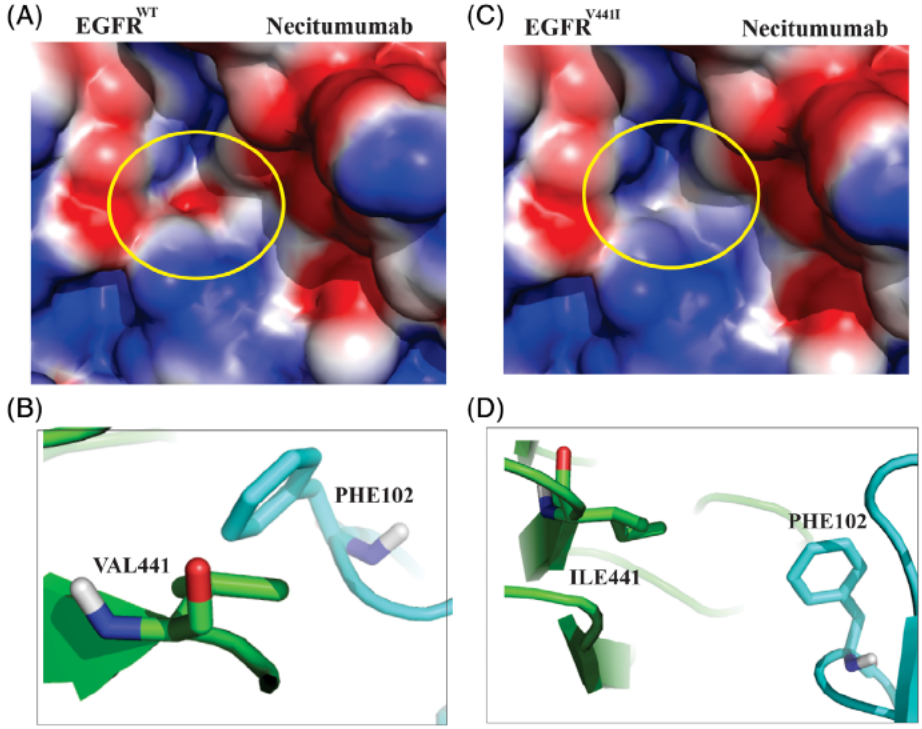

FIGURE 10 Conformation change of the EGFR binding site for Necitumumab because of V441I mutation. A and C are the representation of the interaction surface for $EGFR^{WT}$- and $EGFR^{V441I}$-Necitumumab, respectively. B represents amino acid interaction at the binding sites of $EGFR^{WT}$ in complex with Necitumumab. D represents amino acid interactions at binding sites of $EGFR^{V441I}$ in complex with Necitumumab which the interaction of $EGFR^{WT}$-Necitumumab would disturb by the V441I mutation. EGFR, epidermal growth factor receptor [Color figure can be viewed at wileyonlinelibrary.com]

difference between wild-type and mutant residue makes that the new residue (Tyr) is not in the correct position to make the same hydrogen bond as the original wild-type residue did.

We found that the Val441 residue in EGFR is involved in the interaction with Phe102 of the Necitumumab light chain (Figure 10B). Substitution of Val to Ile at the position of 441 (Figure 10D) in the ectodomain of EGFR, considerably changed the binding site of this receptor from a negatively charged hydrophilic cavity to a positively charged cavity (Figure 10A,C). The electrostatic potential modifications at the binding surface of EGFR may prevent Ile441 for participating in interaction with Phe102 and possibly with the other residues of Necitumumab.

8 DISCUSSION

By the advent of new drugs, especially targeted therapies, the outcome for patients with cancers has improved over the past years. Roughly, 60% of cases with wild-type *RAS* metastatic colorectal tumors benefit from first-line chemotherapy in combination with anti-EGFR antibodies.[19] Likewise, there is much shreds of evidence indicate clinical efficacy of treatment regimens with EGFR-directed antibodies for lung cancer. Unfortunately, the clinical efficacy of EGFR-targeted antibodies is restricted by the development of acquired (secondary) resistance, in most patients at a median of 9-12 months from the start of therapy.[20] Although the mechanism of drug resistance against EGFR-directed small molecule tyrosine kinase inhibitors has been well acknowledged, resistance to anti-EGFR mAbs is poorly understood in oncology. Recent discoveries provided insights into some molecular mechanisms implicated in acquired resistance to anti-EGFR mAbs. These mechanisms include but not limited to; altered key signaling pathways (like RAS-RAF-MEK signal transduction pathway and receptor tyrosine kinase vascular endothelial growth factor receptors [VEGFR] signaling), down-regulation of EGFR by ubiquitination and epitope-changing point mutations in the EGFR ectodomain.[5,6] Unrevealing the molecular basis of such mutations that cause resistance to mAbs could clearly lead to a deeper comprehension of the mutation chemical role and devising of more effective targeted therapies.[21] Thanks to high throughput sequencing technologies, the amount of somatic mutation data in databases (eg, COSMIC) are increasing exponentially. Nonetheless, the majority of mutations available in the databases are yet to be investigated in terms of their burden on structural and functional characteristics of proteins like EGFR.

For this reason, in order to understand the effect of the reported mutations in the ectodomain of EGFR on possible resistance to anti-EGFR mAbs at the molecular level, we modeled mutant EGFRs in complex with mAbs and subsequently performed computational binding free energy calculation for mutant EGFRs to anti-EGFR mAbs including Cetuximab, Panitumumab, Matuzumab, and Necitumumab.

Cetuximab is a chimeric mouse/human IgG1 mAb that binds to EGFR and has demonstrated substantial antitumor activity against colorectal cancer. Panitumumab is a fully humanized IgG2 mAb that is highly selective for EGFR. Both Cetuximab and Panitumumab are currently utilized in the management of metastatic colorectal cancer.[22] Matuzumab is a humanized anti-EGFR mAb that showed therapeutic advantages for colon cancer in the preliminary study.[23] Necitumumab is another anti-EGFR mAb that is a fully humanized IgG1 antibody and showed a modest clinical benefit for treating metastatic nonsmall cell lung cancer.[24]

To inspect the structural consequences of the identified mutations (Table 1), we further modeled the interaction of native and mutant EGFRs with anti-EGFR mAbs. The modeled complexes were subjected to several steps of energy minimization and docking analysis. The results obtained from ClusPro docking server indicate the loss of binding affinity of several mutant EGFRs to the relevant mAb

(Figure 3). An increment of the docking energy is thermodynamically unfavorable in terms of complex stability, therefore in case of each mAbs, we passed the top five complexes with the most positive weighted score to a 50 ns MD simulation.

In the field of computational biophysics, MD is regarded as one of the most widely applied simulation techniques that could calculate binding affinities. In MD, the motions of the atoms that compose proteins are calculated using a simplified model based on Newtonian mechanics. To date, several methodologies for calculating binding affinities from MD simulations have been successfully developed. The molecular mechanics Poisson-Boltzmann surface area (MMPBSA) has become one of the most widely used method for estimating binding free energies. Indeed, MMPBSA popularity is because of its claims to provide a compromise between accuracy and speed.[25,26] In the study, we calculated binding affinities of $EGFR^{WT}$ and mutant EGFRs in complex with mAbs using MMPBSA algorithm.

Our findings suggest that several mutant EGFRs decreased affinity to bind with anti-EGFR mAbs. As a proof-of-principal, two previously described resistance-mediating point mutations S492R, G465R, have been identified by our approach as mutations abrogated antigen-antibody interaction. Herein, we considered such mutations as resistance conferring.

We found that the $EGFR^{S492R}$ mutant loosed its affinity to bind to Cetuximab in comparison to $EGFR^{WT}$ (Δbinding affinity = +975.04 kJ/mol). Also $EGFR^{S492R}$ -Cetuximab showed overall greater RMSD scores as compared to $EGFR^{WT}$ -Cetuximab, resulting in a backbone RMSD of $\sim$0.32 and $\sim$0.22 nm, respectively, at the end of the simulation. Due to a difference in charge between the Ser and Arg amino acid, S492R mutation would introduce positive potential in the interaction surface of $EGFR^{S492R}$ and therefore it may cause repulsion between residues critical for binding to Cetuximab. Overall these findings evidenced that EGFR harboring S492R mutation significantly loss it affinity to Cetuximab. So this mutation may confer resistance to Cetuximab. In contrast, we found that $EGFR^{S492R}$ showed normal affinity as $EGFR^{WT}$ does to other anti-EGFR mAbs particularly Panitumumab. Until recently, no clear therapeutic differences have been acknowledged between Cetuximab and Panitumumab. In 2012, Montagut et al.[6] attempted to know the problem of acquired resistance to Cetuximab that virtually develops in all patients received this mAb.[27] They realized that prolonged in vitro exposure of a Cetuximab-sensitive human colorectal cancer cell line to Cetuximab, induced resistance to this mAb. The Cetuximab-resistant cells harbored S492R mutation in the EGFR binding domain that abrogates Cetuximab binding to EGFR. Interestingly, these S492R EGFR Cetuximab-resistant cells remained to be sensitive to Panitumumab. It implied that this mAb must bind to a different EGFR epitope from the one bound by Cetuximab. In agreement with these findings, our results showed that S492R mutation did not change Panitumumab affinity to EGFR, dramatically.

The mutation G465R is another example of secondary point mutation that confers resistance to anti-EGFR therapies primarily Panitumumab.[7] In our analysis, we identified that this mutation caused a decrease in Panitumumab binding affinity to the EGFR (Table 3). In 2015, Braig et al.[7] reported that acquired resistance to Panitumumab was associated with the emergence of G465R mutation in the EGFR ectodomain. Moreover, they identified that this mutation may also mediate resistance to Cetuximab in preclinical samples. However, we found no significant adverse consequences for this mutation on Cetuximab interaction with EGFR.

In the case of Matuzumab, we found no mutation that substantially deteriorates binding affinity of this mAb to EGFR. It has previously been shown that the epitope for Matuzumab is distinct from the EGFR ligand binding region and also from the Cetuximab epitope.[28] Matuzumab attaches mostly to a buried loop (amino acids 454-464) that precedes the most C-terminal strand of the EGFR ectodomain.[28] One explanation for that why our analysis failed to find a mutation or mutations that adversely affect Matuzumab binding to EGFR, maybe the unusual binding fashion of this mAb to EGFR. Conclusively, the residues affected by the mutations presented in Table 1, are supposed to be different from hot spot residues for Matuzumab binding to EGFR.

We identified that the $EGFR^{V441I}$ mutant has the lowest affinity to bind to both Cetuximab and Necitumumab in comparison with $EGFR^{WT}$. This could be partially explained by the fact that these two mAbs have been shown to interact with EGFR via the same EGFR epitopes.[28] Accordingly, it is conceivable that V441I could lead to cross-resistance to both Cetuximab and Necitumumab.

It is plausible that a number of limitations could have influenced the results obtained. In the presented study we assessed the mutations that were available in COSMIC database v85. Newer versions provide a more comprehensive list of mutations waited to be analyzed. One should bear in mind that molecular docking and MD simulation have limitations as any other technique, so the relevant findings should be interpreted with care. In antibody-antigen docking the important challenge is the less favorable desolvation free energies and more planar interfaces of interacting components in comparison with other protein-protein complexes. Also concerns about rigid-body docking method implemented into the ClusPro server worth to be mentioned here.[29] Theoretically, flexible docking method considers all possible structural modifications and has more realistic prediction than rigid-body docking. However, evaluation of all possible conformational modifications is excessively time-consuming and computation demanding in research. Nevertheless, the majority of the ClusPro developers effort has been directed toward solving presenting flexibility or softness in the rigid-body search and developing a scoring function that distinguishes efficiently between the correct docking solution and the lots of false positives that the search brings up this method considers the molecules as rigid objects.[13,30] In the case of MD simulation, it has some inherent limitations, particularly regarding the force field accuracy. Even with the significant improvement in recent years, still, a deviation from experimental data is evident in respect to MD force filed.

This study was aimed at identifying mutations that contribute to acquire resistance against anti-EGFR mAbs (Cetuximab, Panitumumab, Matuzumab, and Necitumumab). To this aim, we used the COSMIC database data on the somatic mutations within the EGFR ectodomain and performed molecular docking and MD simulation to find candidate mutations. The docking poses of the five top complexes of mutant EGFRs with relevant mAb, were further validated by the MD simulation

as well as MMPBSA free energy calculation. Overall data evidenced that the mutants $EGFR^{S492R}$ and $EGFR^{V441I}$ in complex with Cetuximab, $EGFR^{R377S}$ and $EGFR^{S447Y}$ in complex with Panitumumab, and $EGFR^{V441I}$ in complex with Necitumumab, deteriorated binding affinity of antigen to antibody and also destabilized interface of the complexes. The variants S492R, V441I, R377S, and S447Y are found as EGFR epitope-changing mutation that weakened binding interactions of at least one anti-EGFR mAb with the receptor. Conclusively, we considered such mutations as resistance-conferring mutations. Our findings shed lights on the molecular events that may involve in the acquired resistance to EGFR-targeted therapies. Moreover, the protocol implemented in the current study looks promising to be applied to study mutations that may confer resistance to other anticancer mAbs.

ACKNOWLEDGMENTS

The authors wish to express their gratitude to Dr. Fatemeh Davami and Dr. Hamzeh Rahimi for their support that assisted the research. This research was financially supported by a Pasteur Institute of Iran grant (for Ph.D. thesis of Maryam Tabasinezhad, grant number: BP 9146).

CONFLICT OF INTEREST

The authors do not have any conflict of interest to declare.

ORCID

Hamid Ghaedi https://orcid.org/0000-0002-5034-0586

REFERENCES

1. Mendelsohn J. The epidermal growth factor receptor as a target for cancer therapy. *Endocr Relat Cancer*. 2001;8(1):3-9.
2. Martinelli E, De Palma R, Orditura M, De Vita F, Ciardiello F. Anti-epidermal growth factor receptor monoclonal antibodies in cancer therapy. *Clin Exp Immunol*. 2009;158(1):1-9.
3. Sheng J, Yang YP, Zhao YY, et al. The efficacy of combining EGFR monoclonal antibody with chemotherapy for patients with advanced nonsmall cell lung cancer: a meta-analysis from 9 randomized controlled trials. *Medicine*. 2015;94(34):e1400.
4. Quatrale AE, Petriella D, Porcelli L, et al. Anti-EGFR monoclonal antibody in cancer treatment: in vitro and in vivo evidence. *Front Biosci*. 2011;16:1973-1985.
5. Van Emburgh BO, Sartore-Bianchi A, Di Nicolantonio F, Siena S, Bardelli A. Acquired resistance to EGFR-targeted therapies in colorectal cancer. *Mol Oncol*. 2014;8(6):1084-1094.
6. Montagut C, Dalmases A, Bellosillo B, et al. Identification of a mutation in the extracellular domain of the epidermal growth factor receptor conferring cetuximab resistance in colorectal cancer. *Nat Med*. 2012;18(2):221-223.
7. Braig F, Marz M, Schieferdecker A, et al. Epidermal growth factor receptor mutation mediates cross-resistance to panitumumab and cetuximab in gastrointestinal cancer. *Oncotarget*. 2015;6(14):12035-12047.
8. Forbes SA, Beare D, Boutselakis H, et al. COSMIC: somatic cancer genetics at high-resolution. *Nucleic Acids Res*. 2017;45(D1):D777-d783.
9. Apweiler R, Bairoch A, Wu CH, et al. UniProt: the universal protein knowledgebase. *Nucleic Acids Res*. 2004;32(Database issue):D115-D119.
10. Berman HM, Westbrook J, Feng Z, et al. The Protein Data Bank. *Nucleic Acids Res*. 2000;28(1):235-242.
11. Abraham MJ, Murtola T, Schulz R, et al. GROMACS: High performance molecular simulations through multi-level parallelism from laptops to supercomputers. *SoftwareX*. 2015;1:19-25.
12. Kozakov D, Hall DR, Xia B, et al. The ClusPro web server for protein-protein docking. *Nat Protoc*. 2017;12(2):255-278.
13. Vajda S, Yueh C, Beglov D, et al. New additions to the ClusPro server motivated by CAPRI. *Proteins*. 2017;85(3):435-444.
14. Vaught A. Graphing with Gnuplot and Xmgr: two graphing packages available under linux. *Linux J*. 1996;1996(28es):7.
15. Miller BR III, McGee TD Jr, Swails JM, Homeyer N, Gohlke H, Roitberg AE. MMPBSA. py: an efficient program for end-state free energy calculations. *J Chem Theor Comput*. 2012;8(9):3314-3321.
16. Kumari R, Kumar R, Lynn A. g mmpbsa a GROMACS tool for high-throughput MM-PBSA calculations. *J Chem Inf Model*. 2014;54(7):1951-1962.
17. Jurrus E, Engel D, Star K, et al. Improvements to the APBS biomolecular solvation software suite. *Protein Sci*. 2018;27(1):112-128.
18. Dolinsky TJ, Nielsen JE, McCammon JA, Baker NA. PDB2PQR: an automated pipeline for the setup of Poisson-Boltzmann electrostatics calculations. *Nucleic Acids Res*. 2004;32(Web Server):W665-W667.
19. Bokemeyer C, Bondarenko I, Makhson A, et al. Fluorouracil, leucovorin, and oxaliplatin with and without cetuximab in the first-line treatment of metastatic colorectal cancer. *J Clin Oncol*. 2009;27(5):663-671.
20. Bokemeyer C, Van Cutsem E, Rougier P, et al. Addition of cetuximab to chemotherapy as first-line treatment for KRAS wild-type metastatic colorectal cancer: pooled analysis of the CRYSTAL and OPUS randomised clinical trials. *Europ J Cancer*. 2012;48(10):1466-1475.
21. Bardelli A, Janne PA. The road to resistance: EGFR mutation and cetuximab. *Nat Med*. 2012;18(2):199-200.
22. Buch I, Ferruz N, De Fabritiis G. Computational modeling of an epidermal growth factor receptor single-mutation resistance to cetuximab in colorectal cancer treatment. *J Chem Inf Model*. 2013;53(12):3123-3126.
23. Seiden MV, Burris HA, Matulonis U, et al. A phase II trial of EMD72000 (matuzumab), a humanized anti-EGFR monoclonal antibody, in patients with platinum-resistant ovarian and primary peritoneal malignancies. *Gynecol Oncol*. 2007;104(3):727-731.
24. Thakur MK, Wozniak AJ. Therapy. Spotlight on necitumumab in the treatment of non-small-cell lung carcinoma. *Lung Cancer*. 2017;8:13.
25. Massova I, Kollman PA. Computational alanine scanning to probe protein protein interactions: a novel approach to evaluate binding free energies. *J Am Chem Soc*. 1999;121(36):8133-8143.
26. Kollman PA, Massova I, Reyes C, et al. Calculating structures and free energies of complex molecules: combining molecular mechanics and continuum models. *Acc Chem Res*. 2000;33(12):889-897.
27. Bardelli A, Siena S. Molecular mechanisms of resistance to cetuximab and panitumumab in colorectal cancer. *J Clin Oncol*. 2010;28(7):1254-1261.
28. Schmiedel J, Blaukat A, Li S, Knochel T, Ferguson KM. Matuzumab binding to EGFR prevents the conformational rearrangement required for dimerization. *Cancer Cell*. 2008;13(4):365-373.
29. Brenke R, Hall DR, Chuang G-Y, et al. Application of asymmetric statistical potentials to antibody protein docking. *Bioinformatics*. 2012;28(20):2608-2614.
30. Janin J, Henrick K, Moult J, et al. CAPRI: a critical assessment of predicted interactions. *Proteins*. 2003;52(1):2-9.